

Laser-Induced Abnormal Cryogenic Magnetoresistance Effect in a Corbino Disk

Xinyuan Dong,^{1,2} Diyuan Zheng,^{1,2} Meng Yuan,^{1,2} Yiru Niu,^{1,2} Binbin Liu,^{1,2} and Hui Wang^{1,2,*}

¹State Key Laboratory of Advanced Optical Communication Systems and Networks, School of Physics and Astronomy, Shanghai Jiao Tong University, 800 Dongchuan Road, Shanghai 200240, People's Republic of China

²Key Laboratory for Thin Film and Microfabrication Technology of the Ministry of Education, Research Institute of Micro/Nano Science and Technology, Shanghai Jiao Tong University, 800 Dongchuan Road, Shanghai 200240, People's Republic of China



(Received 7 September 2019; revised manuscript received 27 April 2020; accepted 1 June 2020; published 19 June 2020)

The geometric magnetoresistance effect in semiconductors has remained a heated discussion for many years. However, there are few reports on laser-triggered geometric magnetoresistance in traditional structures. In this work, we use a laser to change the carrier concentration to obtain a large magnetoresistance (212.6%) under a low magnetic field (1 T) at 150 K in a Corbino disk with Co-Ag films. One unanticipated finding is that the large positive magnetoresistance does not change monotonously with temperature, which is different from previous research. Theoretical calculation reveals that the interaction among a photogenerated carrier, bending of the current path, and magnetic nanoparticles in low temperature improves the magnetoresistance in a Corbino disk. These findings reveal an important strategy for creating laser-triggered nanoscale magnetoresistance devices, while presenting a wide range of possibilities for exploring the dependence of photogenerated carriers on temperature under magnetic field.

DOI: 10.1103/PhysRevApplied.13.064050

I. INTRODUCTION

The geometric magnetoresistance (MR) effect [1,2] in nanoscale films has attracted increasing research attention since its discovery [3,4], which is widely used in accurate measurement of carrier concentration [5–7], evaluation of transferred electron device performance [8], high magnetic field sensors [9], current sensors [10], and other fields [11]. A Corbino disk is a quintessential structure to investigate the geometric magnetoresistance effect thoroughly since it can eliminate Hall voltage. Considerable research efforts have been devoted to explain the underlying mechanism of the geometric magnetoresistance effect, which can be attributed to the bending of the current path and uneven carrier distribution [12–14]. However, using a laser to change the carrier concentration and mobility is rarely involved in these studies. Moreover, relatively little attention has been paid to the temperature dependence of the effect, despite its importance for the selection of mechanisms and the development of a microscopic theory of geometric magnetoresistance.

Previously, our group reported a large laser-triggered positive magnetoresistance in a Corbino disk of Cu/SiO₂/Si [15]. With the combined application of laser and magnetic field, the magnetoresistance is significantly improved by more than 60 times compared with other research

[16,17] at the same magnetic field (1 T). On the basis of our previous research, this work investigates the laser-triggered geometric magnetoresistance effect in Co-Ag films, especially to further explore the temperature response of this effect. Thin films consisting of cobalt nanoparticles embedded in a silver matrix are attractive for magnetoresistive research. The phase diagram indicates there is very limited mutual solubility of Co with Ag, which offers the possibility of heterogeneity [18,19]. Experimental results show the laser-triggered magnetoresistance of Co-Ag films can reach 212.6% and 8.2% at 150 K and room temperature under a magnetic field of 1 T, respectively. The magnetoresistance is significantly enhanced compared with previous studies under the same circumstances (1 T magnetic field) [12,15,18,20]. We also notice, most surprisingly, that the magnetoresistance does not change monotonously with temperature, unlike the monotonous rise in magnetoresistance of granular films caused by scattering with a decreasing temperature [19]. This research extends the knowledge into the geometric magnetoresistance mechanisms induced by laser and temperature, while opening the door to the possibilities in temperature sensors and magnetoresistance devices.

II. FABRICATION AND METHODS

We fabricate Co-Ag composite films on the doped *n*-type Si (111) wafers (approximately 0.3 mm thickness, 20–50 Ωcm resistivity) with a native ultrathin oxide layer

*huiwang@sjtu.edu.cn

approximately 1.2 nm thick on one side. Co-Ag films are deposited by co-sputtering of Co and Ag targets (purity better than 99.9%) using dc magnetron sputtering from two confocal sputter magnetron guns at room temperature. The whole sputtering process is in an argon pressure of 0.78 Pa, and the base pressure of the vacuum system is better than 3.8×10^{-4} Pa. The dc power of cobalt and silver is fixed at 10 and 20 W, respectively. The deposition rate is 3.2 \AA s^{-1} , which is determined by the step profiler on thick calibration samples fabricated under the same condition. A ring-shape mask is utilized to deposit the film. First, the ring groove is covered by the mask and deposited for 145 s. Then, the mask is removed, and the whole part is deposited for 5 s. Counting with the deposition rate, the electrode layer of 48 nm Co-Ag alloy is deposited on center and peripheral areas of the Si substrate, as annotated in Fig. 1(a). The annular region between two electrodes is 1.6 nm (nominal thickness) superthin Co-Ag composite films. We switch the dc power of the Co target to regulate the content of cobalt in the samples. The compositional distribution of the alloy film is further investigated by energy dispersive spectroscopy (EDS).

Figure 1(a) shows a representative schematic diagram of a Corbino disk, where r_a is the radius of center region and r_b is the outer radius of the ring. The width of the

ring groove is defined as $r_b - r_a$. During the experiment, the ring width of all samples is maintained at 1.5 mm. Electrodes A and B of alloying indium (less than 1 mm in diameter) are pressed on the central and peripheral bulk Co-Ag areas, respectively. Figures 1(b) and 1(c) show SEM images of the two different regions, and the inset shows the corresponding EDS spectra. SEM images recorded at high magnification clearly show that the as-deposited films consist of a bulk region with uniform shapes [Fig. 1(b)] and nanoparticles [Fig. 1(c)].

In the experimental process, electrode A is irradiated by a 635-nm, 3-mW laser focused on a roughly 50- μm diameter spot continuously, and without any background light illumination. We measure the magnetoresistance using the two-probe method in a vacuum cavity with a pressure of 1.0×10^{-4} Pa, and the chamber temperature ranged from 20 to 300 K in the presence of a magnetic field in the z -axis direction varying up to 1 T. The chamber temperature is regulated by helium compressors and a temperature controller, and the resistance is determined using the Keithley 4200-SCS Semiconductor Characterization System. The magnetoresistance is defined as

$$\Delta R/R_0 = [(R_H - R_0)/R_0] \times 100\%. \quad (1)$$

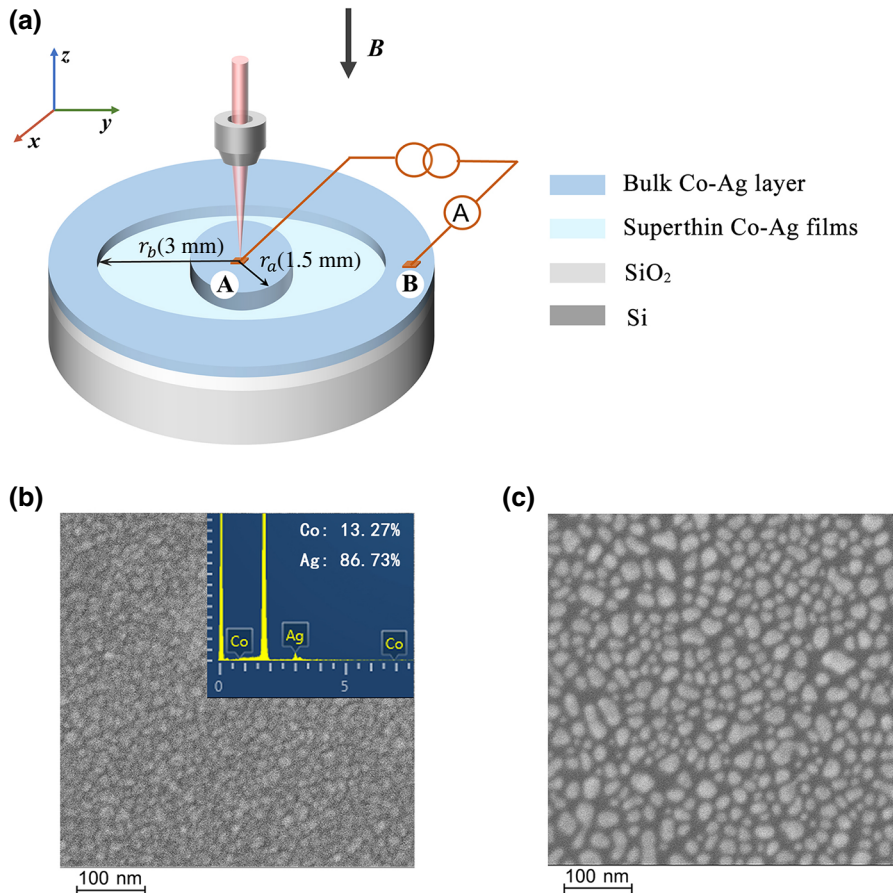


FIG. 1. (a) Schematic diagram of Corbino structure with Co-Ag/SiO₂/Si and the experimental measurement method. (b) SEM image of the bulk Co-Ag layer. Inset shows the corresponding EDS spectra. (c) SEM image of the annular groove region where superthin Co-Ag films are deposited.

Here, R_H represents the resistance with the external magnetic field applied, and R_0 is the resistance in the absence of magnetic field.

III. RESULTS AND DISCUSSION

Figure 2(a) shows the I - V curves of the Co-Ag/SiO₂/Si sample between electrode A and B under different conditions at 20 K (equipment limit). We define the forward-sweep voltage to represent the case where electrode A is the anode and B is the cathode. The original I - V curve (i.e., without laser irradiated and magnetic field applied) is symmetrical, and the sample is in a high-resistance state. However, when a fixed 635-nm laser is applied perpendicularly to electrode A, the resistance is significantly reduced. Most surprisingly, the I - V curve exhibited extreme asymmetry, which suggested a laser-induced polar resistance effect. This bipolar resistance effect has been reported in our previous research, which can be attributed to diffusion and scattering of carriers based on Schottky

barriers [15]. On this basis, we apply a 1-T magnetic field perpendicular to the sample, the I - V characteristic as indicated by the blue line in Fig. 2(a). The resistance of the sample increases observably under the combined effect of laser and magnetic field. Nevertheless, when the laser is removed, the I - V characteristic is almost the same as the original curve. From the results we can conclude that the laser plays an indispensable role in the effect.

In order to further investigate the effect of temperature and magnetic field on magnetoresistance, we fix the laser position and change the ambient temperature, and measure the magnetoresistance under different magnetic fields. The MR values are calculated by Eq. (1). Figure 2(b) shows MR data of the Co-Ag/SiO₂/Si sample versus magnetic field for various temperatures. As the magnetic field increases, the MR value is drastically promoted, which is in consonance with the work we have reported before [15]. Besides, the magnetoresistance in a Corbino disk structure presents excellent symmetry to the direction of applied magnetic field. As for temperature dependence, the MR

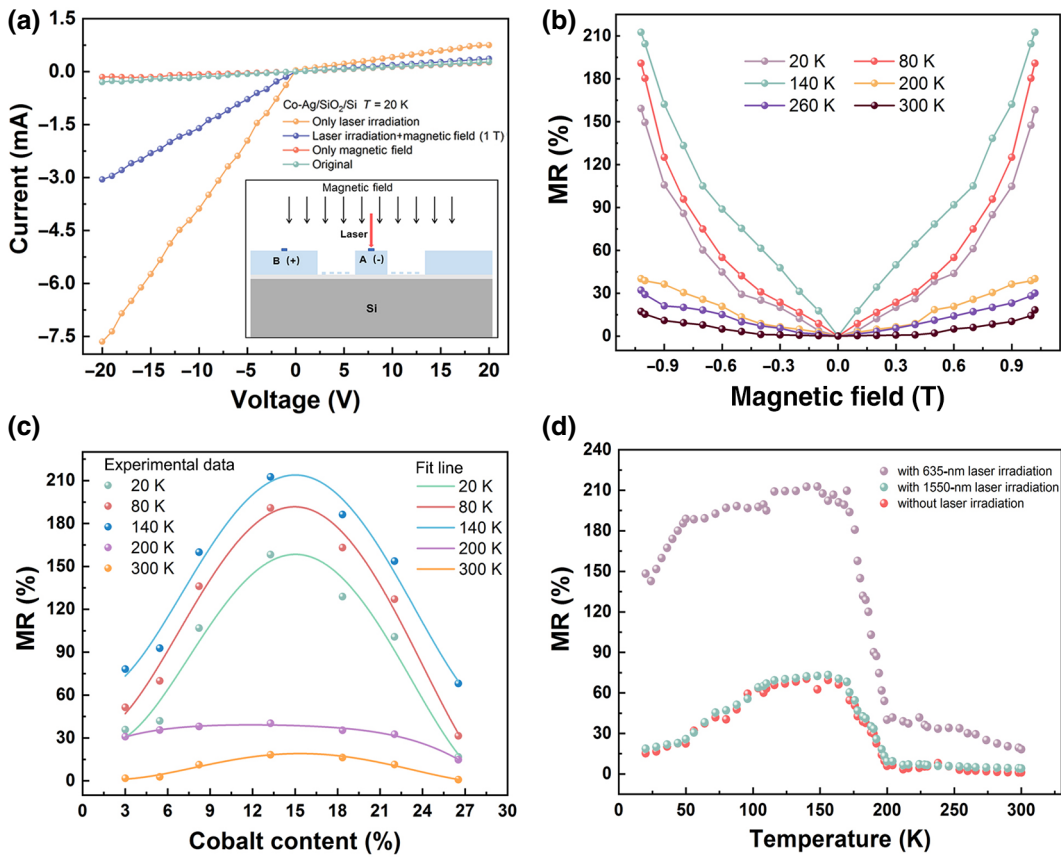


FIG. 2. (a) I - V curves of the Co-Ag/SiO₂/Si sample with different laser and magnetic field conditions. The ambient temperature is set to 20 K, and measurement details are shown in the inset. A fixed 635-nm, 3-mW laser on a roughly 50- μ m diameter spot perpendicular to electrode A. (b) MR ratio of the Co-Ag/SiO₂/Si sample as a function of magnetic field at different temperatures. (c) The Co-Ag/SiO₂/Si sample's MR ratio versus cobalt content as a function of temperature. The applied magnetic field is fixed at 1 T and the measurement condition is identical to before. (d) The dependence of the Co-Ag/SiO₂/Si sample's MR on temperature with different laser conditions. The measurement condition is the same compared to before (with a 1-T magnetic field and 635-nm laser applied).

values increase with the increasing temperature and grow up to the maximum when the temperature is 150 K, and then decrease sharply above 170 K. We obtain a large magnetoresistance of 212.6% at 150 K, only 1-T magnetic field, which is comparable to other research.

To gain deeper insight related to the laser-triggered MR effect in Co-Ag films, a systematic study has been carried out in Co-Ag/SiO₂/Si samples with cobalt content varying from 3.01% to 26.53%. The cobalt content is governed by sputtering time and power, and determined by energy dispersive spectroscopy. We prepare samples with the same nominal Co-Ag thickness but different cobalt contents. During the experiment, the applied magnetic field is fixed at 1 T and the samples are irradiated by a 635-nm laser continuously. A clear dependence of MR on the cobalt content is observed [Fig. 2(c)]. The same general trend is found at different temperatures: the MR value increases with the cobalt content up to a maximum and then drops off with the higher cobalt content.

As is widely known, a laser may cause the temperature change in the place of irradiation, and further leading to the apparition of temperature gradients. In order to eliminate the possibility that the local temperature change caused by a laser contributes to the magnetoresistance, we measure the dependence of MR on temperature with different laser conditions in a 1-T magnetic field. As annotated in Fig. 2(d), MR values present the same tendency with temperature changes under different illumination conditions. When the temperature is below 150 K, the magnetoresistance increases slowly with temperature. With temperature increasing from 150 to 200 K, the magnetoresistance value is drastically reduced. Once the temperature is greater than 200 K, the magnetoresistance decreases very slowly with increasing temperature. Besides, the MR effect with 1550-nm laser irradiation almost has no change compared with the case with no laser irradiation, but it is greatly enhanced with 635-nm laser irradiation, indicating the local temperature change caused by the laser does not contribute to the magnetoresistance effect.

The influence of magnetic materials on magnetoresistance is non-negligible. To further investigate the magnetism of samples, magnetic hysteresis, the field cooled (FC), and the zero field cooled (ZFC) are employed. Figure 3(a) shows the full hysteresis loops of the magnetization measured at room temperature on the Co-Ag (nominal thickness, 1.6 nm, and 13.27% Co) sample for parallel (||) and perpendicular (⊥) to film plane orientations of the applied magnetic field. The inset shows the enlarged image of the M - H curve corresponding to H perpendicular (⊥) to the film, and the sample exhibits negligible coercivity force (16.8 Oe). It is found that the two M - H curves could not reach saturation even at the maximum magnetic field of 1.5 T, which clearly indicates the presence of superparamagnetic particles [21]. And the easy axis of the nanoparticles is out of plane. To confirm

the superparamagnetic behavior, we measure the ZFC and FC data in the temperature range 2–400 K, as shown in Fig. 3(b). For samples with 13.27% Co, the $M_{\text{ZFC}}(T)$ curve exhibits the maximum at $T_B \sim 170$ K, while the $M_{\text{FC}}(T)$ curve decreases monotonously with the increasing temperature. Such magnetic properties indicate the superparamagnetic character of the Co nanoparticles in our samples [22]. Besides, the blocking temperature in the sample with 13.27% Co is larger than the sample with 8.22% Co, which suggests the increase in particle size. Moreover, the FC curves suggest the absence of cobalt oxide. Because CoO is antiferromagnetic, the magnetization of FC curve will exhibit a sharp drop above the Neel temperature of 290 K. However, this is not observed in our samples.

Magnetic measurements of the samples are carried out to determine whether the Co-Ag materials contribute greatly to magnetoresistance. Figure 3(c) shows the MR ratio as a function of temperature in Co-Ag/SiO₂/Si with ordinary structure (without Corbino geometry). The nominal thickness of Co-Ag film is fixed at 1.6 nm, which is the same as the thickness in a Corbino disk. And the content of cobalt is 13.27%. As can be seen in Fig. 3(c), the magnetoresistance values are quite small in the absence of laser, and the temperature dependence of MR is consistent with previous researches [19,23]. However, the magnetoresistance is considerably improved when the laser is applied. And the temperature dependence is completely different from that without laser. With the temperature increasing from 20 to 170 K, the laser-triggered MR declines slowly. Once the temperature is higher than 170 K, the laser-triggered MR ratio decreases sharply until 230 K. Obviously, the magnetic material has a certain contribution to the magnetoresistance below T_B (170 K), but it makes little contribution once the temperature is higher than T_B . We think these results can be attributed to the transition from ferromagnetism to superparamagnetism, which involves a transition from ordered to disordered orientations of the electron spins. The neighboring islands tend to be parallel aligned by the external field and reduce the resistance in the absence of laser, thereby, the negative magnetoresistance. But when the laser is applied, the photogenerated carriers play a vital role in the magnetoresistance. In the diffusion process of carriers, electrons in Co-Ag also may recombine with holes in silicon. And the carrier recombination rate is affected by scattering. When the temperature is below T_B , the particles exhibit ferromagnetism. Under the applied magnetic field, the spin-dependent scattering of conducting electrons contribute to the increase of photogenerated carrier recombination rate, thereby, the increased resistance and positive magnetoresistance. But when the temperature is higher than T_B , the thermal energy can disrupt the magnetic moment, thereby weakening the magnetism, which contributes little to the magnetoresistance.

For comparison, we also measure the temperature dependence of laser-triggered MR in Corbino disks with

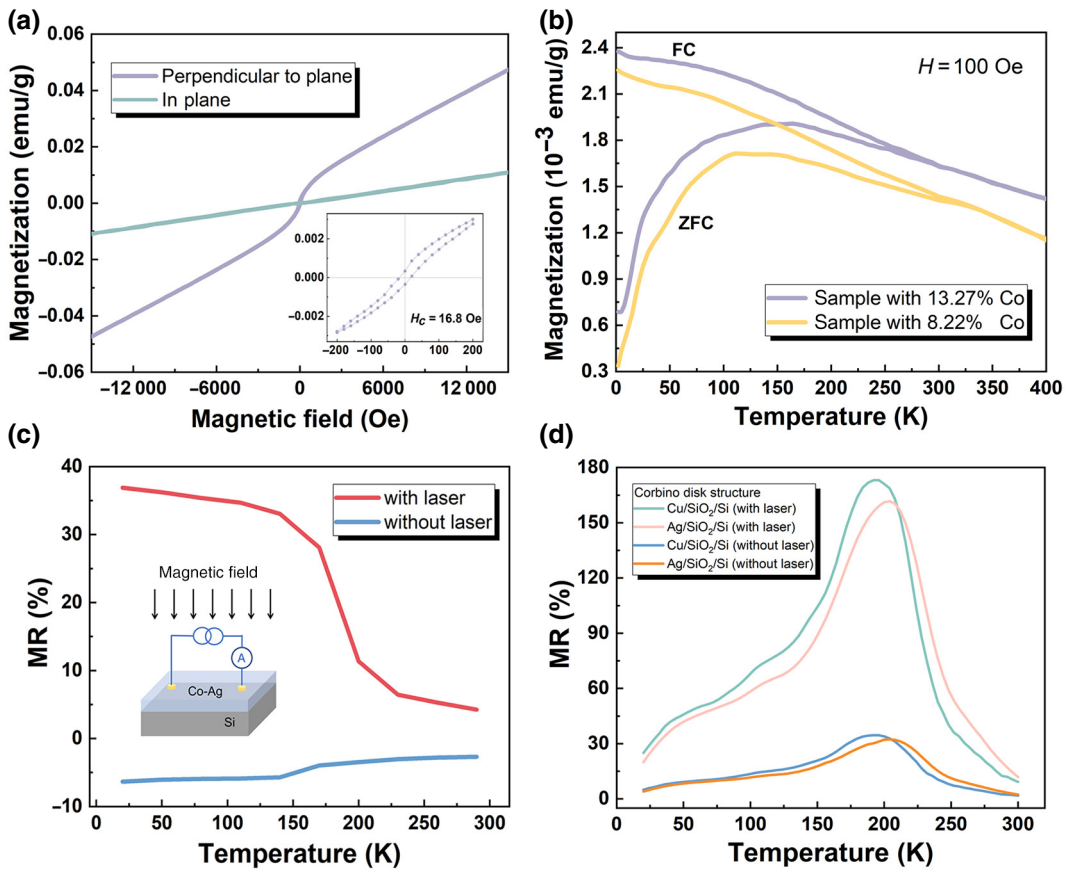


FIG. 3. (a) M - H hysteresis loops corresponding to H parallel (\parallel) and perpendicular (\perp) to film measured at room temperature for the Co-Ag (nominal thickness, 1.6 nm, and 13.27% Co) sample. (b) Temperature dependence of magnetization in Co-Ag samples with different Co contents, in the ZFC and FC protocols in the presence of magnetic field of 100 Oe. (c) The MR ratio as a function of temperature in Co-Ag/SiO₂/Si with ordinary structure (without Corbino geometry). The nominal thickness of the Co-Ag film is 1.6 nm and the content of cobalt is 13.27%. The inset shows the measurement method. (d) Dependence of laser-triggered MR ratio on temperature with nonmagnetic materials in Corbino disks. The width of the ring groove is fixed at 1.5 mm, and the thickness of metal kept consistent.

nonmagnetic materials, as shown in Fig. 3(d). Both of the samples show similar nonmonotonic temperature dependence. Compared with the magnetoresistance in magnetic materials shown in Fig. 2(d), there is a striking difference when the temperature is quite low. The magnetoresistance in magnetic materials is much larger than that in nonmagnetic materials.

To explain these phenomena, we propose a model based on the Schottky barrier. The samples contain bulk Co-Ag layers and superthin films, and the Schottky barrier is much lower in the annular groove region, which covered by superthin films [15]. Therefore, the equivalent circuit can be considered as two reverse diodes and a pure resistor, as indicated in Fig. 4 (left). Obviously, the system is in a high-resistance state without laser irradiation. When the laser is applied, a large amount of photogenerated carriers are generated in the silicon substrate. There was a high carrier concentration at the laser spot, so carriers diffuse to the surrounding. [24–26] And photogenerated electrons have

the opportunity to tunnel into the alloy layer. The application of magnetic field brought on the deflection of a carrier motion path under Lorentz force, thereby, the increased resistance (Fig. 4, right).

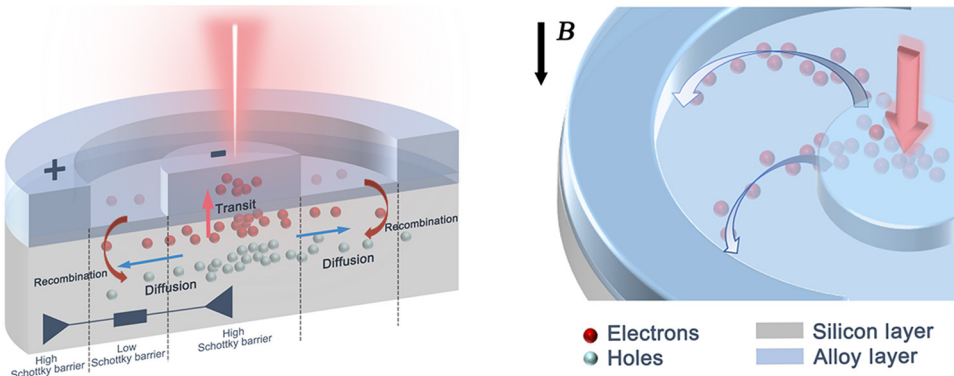
If we suppose the initial resistivity without a laser and magnetic field is ρ_0 , the resistance at position x (i.e., the distance from the laser spot) can be written as [27,28]

$$\rho(x) \approx \rho_0 \left(1 - \frac{n_0}{N_0} + \frac{n_0}{N_0 \lambda} x \right). \quad (2)$$

Here λ is the diffusion length, n_0 and N_0 represent the density of laser-induced electrons and drift carriers at the laser spot, respectively.

In previous research, we have derived the current path formula under the applied magnetic field, which can be written as [15,29]

$$s = \alpha x, \quad (3)$$



here,

$$\alpha = \sqrt{1 + \frac{\mu^2 H^2}{c^2}}, \quad (4)$$

and μ is the carrier mobility, H is the density of magnetic field, and c is a constant in the Gauss unit system. We find that the new parameter α characterizes the current path change caused by magnetic field in the Corbino disk. More simply, α characterizes the extent of motion-path bending. Note that a laser is a prerequisite in the experiment. R_0 represents the resistance with laser irradiation only, and it can be written as a path integral of $\rho(x)$:

$$R_0 = \int_{r_a}^{r_b} \rho(x) dx. \quad (5)$$

However, when the magnetic field is applied, the current path changed, thereby, the resistivity at different positions.

$$R_H = \int_{r_a}^{r_b} \rho(s) ds = \alpha \int_{r_a}^{r_b} \rho(\alpha x) dx. \quad (6)$$

Finally, the laser-triggered magnetoresistance can be written as

$$\Delta R/R_0 \approx \alpha + \frac{(\alpha^2 - \alpha)}{1 + k\lambda \left(\frac{N_0}{n_0} - 1 \right)}. \quad (7)$$

Here $k = 1/(r_a + r_b)$ is a constant. From Eq. (7), we can see the temperature T has an influence on three parameters: λ , N_0/n_0 , and α . The diffusion length λ can be written as [26,30]

$$\lambda = \sqrt{D\tau} \propto T^{-1}, \quad (8)$$

where D is diffusion coefficient affected by temperature. And according to the Boltzmann distribution function, the

FIG. 4. Schematic diagram of photogenerated carriers' movement only laser irradiated (left). The carriers' motion path with the combined effect of laser and magnetic field (right).

carrier concentration satisfies

$$\frac{N_0}{n_0} \propto e^{-\frac{E_C - E_F}{k_0 T}} \propto e^{-\frac{1}{T}}. \quad (9)$$

The parameter α , which measures the current path change caused by magnetic field described in Eq. (4), can be simplified as $\alpha \propto \mu$. Here, μ is the mobility, which can be written as [17]

$$\mu = \frac{q\tau}{m^*}. \quad (10)$$

Here m^* and τ are the effective mass and lifetime of the carrier, respectively. Hence, the MR can be simplified as

$$\Delta R/R_0 \propto \mu(T) \left\{ 1 + \frac{[\mu(T) - 1]T}{e^{-1/T}} \right\}. \quad (11)$$

Here, $e^{-1/T}$ approaches a constant as temperature increases. Therefore, we mainly take the mobility μ into consideration. The scattering processes influence the lifetime, thereby, limiting the mobility. Due to the large carrier density, the thermal vibration of the lattice has a non-negligible influence on the mobility even at low temperature. Therefore, the ionized impurity scattering dominates at low temperatures, where $\mu \propto T^{3/2}$. Apparently, the magnetoresistance increases with the increasing temperature. But as the temperature further rises, the lattice vibration scattering dominates, which satisfies $\mu \propto T^{-3/2}$ [17]. As a result, the magnetoresistance decreases. Similar temperature dependence of magnetoresistance (without laser irradiation) in a Corbino disk has been reported in previous research [17]. According to the above analysis, we conclude that the nonmonotonic temperature dependence of magnetoresistance is mainly due to the change of mobility in Corbino structure. And the laser plays a significant role in generating photogenerated carriers and amplifying magnetoresistance. Under the influence of these factors, the magnetoresistance grows monotonously up to maximum, above which it precipitously decreases.

Besides, taking into account the contribution of magnetic nanoparticles below the blocking temperature T_B ,

the recombination rate of photogenerated carriers increases due to the spin-dependent scattering. As a result, the diffusion length λ decreases. According to Eq. (7), the magnetoresistance is enhanced below T_B , which also explains the reason why the MR effect in magnetic particles is better than nonmagnetic at low temperatures.

As for the cobalt content dependence of MR shown in Fig. 2(c), it can be attributed to changes in particle size. When the concentration of magnetic particles is small, there is less scattering and larger particle spacing, which leads to the small magnetoresistance. Therefore, as the cobalt content is increased, the MR effect is improved. However, as indicated in Fig. 3(b), T_B increases with increasing cobalt content, which suggests the increase in particle size. As the particles grow larger, the surface:volume ratio decreases, which weaken the spin-dependent scattering of conducting electrons [19,31]. As a result, the photogenerated carrier recombination rate decreases, thereby, the magnetoresistance is reduced.

IV. CONCLUSION

In conclusion, we obtain a colossal magnetoresistance effect using a simple laser-triggered method in Corbino disks with Co-Ag films. The temperature dependence of the laser-triggered magnetoresistance effect is investigated in the temperature range from 20 to 300 K. What is surprising is that the dependence of the MR ratio on temperature is nonmonotonic. Moreover, the MR effect is closely associated with the elemental component of samples. We show that the Corbino geometry, diffusion length, and magnetic nanoparticles contribute to the magnetoresistance. This work expands the possibility of design for laser-triggered and temperature-regulated magnetoresistance devices.

ACKNOWLEDGMENTS

We acknowledge the financial support of the National Natural Science Foundation of China under Grants No. 11874041, No. 61574090, No. 11374214, and No. 10974135.

- [1] S. A. Solin, T. Thio, D. R. Hines, and J. J. Heremans, Enhanced room-temperature geometric magnetoresistance in inhomogeneous narrow-Gap semiconductors, *Science* **289**, 1530 (2000).
- [2] C. Wan, X. Zhang, X. Gao, J. Wang, and X. Tan, Geometrical enhancement of low-field magnetoresistance in silicon, *Nature* **477**, 304 (2011).
- [3] G. L. Yuan, J. M. Liu, X. J. Zhang, and Z. G. Liu, Enhanced room-temperature geometric magnetoresistance in a modified van der Pauw disk, *Mater. Lett.* **56**, 0 (2002).
- [4] S. U. Yuldashev, Y. Shon, Y. H. Kwon, D. J. Fu, D. Y. Kim, H. J. Kim, T. W. Kang, and X. Fan, Enhanced positive magnetoresistance effect in GaAs with nanoscale magnetic clusters, *J. Appl. Phys.* **90**, 3004 (2001).

- [5] N. Rodriguez, L. Donetti, F. Gamiz, and S. Cristoloveanu, in 2007 IEEE Int. SOI Conf. (IEEE, 2007), pp. 59–60.
- [6] J. P. Campbell, K. P. Cheung, L. C. Yu, J. S. Suehle, A. Oates, and K. Sheng, Geometric magnetoresistance mobility extraction in highly scaled transistors, *IEEE Electron Device Lett.* **32**, 75 (2011).
- [7] W. Chaisantikulwat, M. Mouis, G. Ghibaudo, C. Gallo, C. Fenouillet-Beranger, D. K. Maude, T. Skotnicki, and S. Cristoloveanu, Differential magnetoresistance technique for mobility extraction in ultra-short channel FDSoI transistors, *Solid State Electron.* **50**, 637 (2006).
- [8] M. Howes, D. Morgan, and W. Devlin, Applications of magnetoresistance measurements in the evaluation of transferred electron device performance, *Phys. Status Solidi A-Appl. Mat.* **41**, 117 (1977).
- [9] W. R. Branford, A. Husmann, S. A. Solin, S. K. Clowes, T. Zhang, Y. V. Bugoslavsky, and L. F. Cohen, Geometric manipulation of the high-field linear magnetoresistance in InSb epilayers on GaAs (001), *Appl. Phys. Lett.* **86**, 202116 (2005).
- [10] S. Ziegler, R. C. Woodward, H. H.-C. Iu, and L. J. Borle, Current sensing techniques: A review, *IEEE Sens. J.* **9**, 354 (2009).
- [11] D. Monsma, J. Lodder, T. J. Popma, and B. Dieny, Perpendicular hot Electron Spin-Valve Effect in a new Magnetic Field Sensor: The Spin-Valve Transistor, *Phys. Rev. Lett.* **74**, 5260 (1995).
- [12] B. Zou, P. Zhou, J. Zou, Z. Gan, C. Mei, and H. Wang, Using laser to trigger a large positive magnetoresistive effect in nonmagnetic Si-based metal-oxide-semiconductor structure, *Appl. Phys. Lett.* **111**, 241103 (2017).
- [13] V. Guttal and D. Stroud, Model for a macroscopically disordered conductor with an exactly linear high-field magnetoresistance, *Phys. Rev. B* **71**, 201304R(201301-201304) (2005).
- [14] M. M. Parish and P. B. Littlewood, Classical magnetotransport of inhomogeneous conductors, *Phys. Rev. B* **72**, 094417 (2005).
- [15] X. Dong, D. Zheng, M. Yuan, P. Zhou, Y. Niu, A. Dong, and H. Wang, Laser-Triggered large magnetoresistance change observed in corbino disk of Cu/SiO₂/Si, *Adv. Electron. Mater.* **5**, 1800844 (2019).
- [16] B. Madon, J. E. Wegrowe, M. Hehn, F. Montaigne, and D. Lacour, Corbino magnetoresistance in ferromagnetic layers: Two representative examples Ni₈₁Fe₁₉ and Co₈₃Gd₁₇, *Phys. Rev. B* **98**, 220405 (2018).
- [17] J. Sun, Y.-A. Soh, and J. Kosel, Geometric factors in the magnetoresistance of n-doped InAs epilayers, *J. Appl. Phys.* **114**, 203908 (2013).
- [18] J. Garcia-Torres, E. Gómez, and E. Vallés, Measurement of the giant magnetoresistance effect in cobalt–silver magnetic nanostructures: Nanowires, *J. Phys. Chem. C* **116**, 12250 (2012).
- [19] A. E. Berkowitz, J. R. Mitchell, M. J. Carey, A. P. Young, D. Rao, A. Starr, S. Zhang, F. E. Spada, F. T. Parker, A. Hutten, et al., Giant magnetoresistance in heterogeneous Cu–Co and Ag–Co alloy films (invited), *J. Appl. Phys.* **73**, 5320 (1993).
- [20] E. Barati and M. Cinal, Gilbert damping in binary magnetic multilayers, *Phys. Rev. B* **95**, 134440 (2017).

- [21] D. Kumar, S. Chaudhary, and D. K. Pandya, Perpendicular magnetic anisotropy and complex magnetotransport behavior of cobalt nanoparticles in silver matrix, *J. Appl. Phys.* **117**, 17C752 (2015).
- [22] T. Jaumann, E. M. M. Ibrahim, S. Hampel, D. Maier, A. Leonhardt, and B. Büchner, The synthesis of superparamagnetic cobalt nanoparticles encapsulated in carbon through high-pressure CVD, *Chem. Vap. Deposition* **19**, 228 (2013).
- [23] A. Gerber, A. Milner, I. Y. Korenblit, M. Karpovsky, A. Gladkikh, and A. Sulpice, Temperature dependence of resistance and magnetoresistance of nanogranular Co-Ag films, *Phys. Rev. B* **57**, 13667 (1998).
- [24] S. Liu, C. Yu, and H. Wang, Colossal lateral photovoltaic effect observed in metal-oxide-semiconductor structure of Ti/TiO₂/Si, *IEEE Electron Device Lett.* **33**, 414 (2012).
- [25] L. Kong, H. Wang, S. Xiao, J. Lu, Y. Xia, G. Hu, N. Dai, and Z. Wang, Integrated properties of large lateral photovoltage and positive magnetoresistance in Co/Mn/Co/c-Si structures, *J. Phys. D: Appl. Phys.* **41**, 052003 (2008).
- [26] B. Zhang, L. Du, and H. Wang, Bias-assisted improved lateral photovoltaic effect observed in Cu₂O nano-films, *Opt. Express* **22**, 1661 (2014).
- [27] D. Zheng, C. Yu, Q. Zhang, and H. Wang, Evaluating nanoscale ultra-thin metal films by means of lateral photovoltaic effect in metal-semiconductor structure, *Nanotechnology* **28**, 505201 (2017).
- [28] C. Yu and H. Wang, Light-Induced bipolar-resistance effect based on metal-oxide-semiconductor structures of Ti/SiO₂/Si, *Adv. Mater.* **22**, 966 (2010).
- [29] D. A. Kleinman and A. L. Schawlow, Corbino disk, *J. Appl. Phys.* **31**, 2176 (1960).
- [30] K. Zhang, H. Wang, Z. Gan, P. Zhou, C. Mei, X. Huang, and Y. Xia, Localized surface plasmon resonances dominated giant lateral photovoltaic effect observed in ZnO/Ag/Si nanostructure, *Sci. Rep.* **6**, 22906 (2016).
- [31] H. Sang, G. Ni, J. H. Du, N. Xu, S. Y. Zhang, Q. Li, and Y. W. Du, Preparation and microstructures of CoAg granular films with giant magnetoresistance, *Appl. Phys. A* **63**, 167 (1996).